

Low-Bias Control of AMB Subject to Voltage Saturation: State-Feedback and Observer Designs

Panagiotis Tsiotras
School of Aerospace Engineering
Georgia Institute of Technology, Atlanta, GA 30332-0150, USA
p.tsiotras@ae.gatech.edu

Murat Arcak
Electrical, Computer and Systems Engineering
Rensselaer Polytechnic Institute
Troy, New York, 12180-3590, USA
arcak@ecse.rpi.edu

Abstract

This paper addresses the problem of low-bias control for an active magnetic bearing (AMB) subject to voltage saturation. Using a generalized complementarity flux condition, a simple, three-dimensional model is used to describe the dynamics of the low-bias mode of operation. Several stabilizing controllers are derived by applying recent results from nonlinear control theory.

1 Introduction

It is envisioned that future commercial and military spacecraft will have an unprecedented degree of autonomy made possible by increased on-board processing speed and memory capabilities. This increase in on-board processing, autonomous sensing and communication capabilities translates directly to large requirements for on-board available power. Traditional chemical batteries have several limitations stemming from their inherent unreliability, low depth of discharge, heavy weight, limited life, etc.

An alternative to the chemical batteries for energy storage and power generation for future spacecraft has been proposed in recent years, namely, that of electromechanical (e.g., flywheel) batteries [9]. Taking into consideration that most orbiting spacecraft already incorporate moving wheels (e.g., reaction, momentum wheels, CMG's) for attitude control, the prospect of using these spinning wheels to also store energy seems natural and appealing. Several technical challenges need to be overcome, however, before efficient flywheels become a part of a standard spacecraft power subsystem. One such major challenge is the design of flywheels supported on low-loss active magnetic bearings (AMB's).

Efficient operation of flywheel electromechanical batteries necessitates minimization of energy losses (mechanical and other). Mechanical losses (friction) are reduced via the use of AMB's. Ohmic and eddy current losses on the other hand (which can be quite significant for high-speed flywheels) can be reduced by minimizing or eliminating the bias current during AMB opera-

tion [4, 7]. However, owing to the nonlinear flux/force characteristic reduction or elimination of the bias current leads to a nonlinear region which is dominated, among other things, by slew-rate force limitations close to the origin [2]. These limitations manifest themselves as saturation constraints on the power amplifier voltage driving the coils of the electromagnets. The problem of designing low-bias control laws for AMB's subject to saturation constraints is thus a nontrivial nonlinear control problem.

In this paper we use recent results from the theory of saturating control to design stabilizing control laws for AMBs in low bias operation, subject to voltage saturation constraints. The main design tools in this framework are passivity and the asymptotic small-gain theorem and nested saturation designs due to Teel [13]. We present three low-bias designs for an AMB. The first two designs ensure global asymptotic stability in case of soft saturation constraints. The third design ensures global asymptotic stability in case of hard voltage saturation constraints.

All controllers proposed in this work require flux feedback. Since flux is not easily measurable in practice, a nonlinear observer is designed and incorporated in certainty-equivalence implementations of the state-feedback control laws. The stability proof of this certainty-equivalence scheme is given for each of the three control laws. Numerical examples demonstrate the theoretical developments.

2 Modeling of an AMB in Low Bias Mode

The simplified AMB model used in this paper consists of two identical electromagnets, which are used to move a rotor of mass m in one dimension. To regulate the position x of the mass to zero, the control designer uses the voltage inputs of the electromagnets, V_1 and V_2 , in order to exert attractive forces on the rotor; see Fig. 1. Neglecting gravity, the total force generated by each electromagnet is given by [10]

$$F_i = \frac{\Phi_i^2}{\mu_o A_g}, \quad i = 1, 2 \quad (1)$$

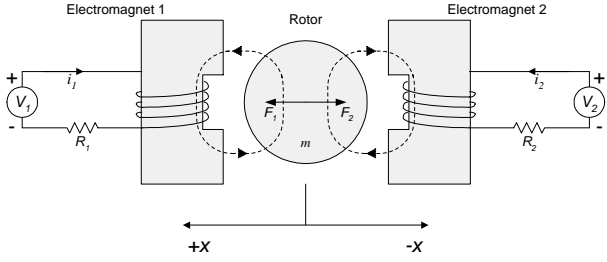


Figure 1: Simplified AMB geometry.

where Φ_i is the total magnetic flux of the i -th electromagnet, A_g is the cross sectional area of the airgap at the pole, and μ_o is the permeability of free space ($= 1.25 \times 10^{-6}$ H/m). In non-zero bias operation we distinguish the total magnetic flux into the bias flux Φ_0 and the perturbation (control) flux $\Delta\Phi_i$ generated by the i -th electromagnet. The total flux generated by the i -th electromagnet is then $\Phi_i = \Phi_0 + \Delta\Phi_i$, ($i = 1, 2$). Enforcing the following *generalized complementary flux condition* (gfcf) on the *perturbation flux* $\Delta\Phi_i$ [14]

$$\begin{aligned} \Delta\Phi_1 &= \Delta\Phi, & \Delta\Phi_2 &= 0 & \text{when } \Delta\Phi &\geq 0 \\ -\Delta\Phi_2 &= \Delta\Phi, & \Delta\Phi_1 &= 0 & \text{when } \Delta\Phi &\leq 0 \end{aligned} \quad (2)$$

one obtains the equation for the dynamics of the system as

$$\ddot{x} = \frac{1}{\kappa} (\Delta\Phi |\Delta\Phi| + 2\Phi_0 \Delta\Phi), \quad (3)$$

where $\kappa = m\mu_o A_g$. The gfcf operation constraint tries to reduce the overall flux, thus ensuring smaller power losses.

When the bias flux is taken to be zero ($\Phi_0 = 0$) our gfcf model reduces to the standard *complementary flux condition* (cfc) operation mode [14].

Using the gfcf (2) Faraday's law gives the electrical dynamics simply as¹

$$\dot{\Phi}_i = \Delta\dot{\Phi}_i = \frac{V_i}{N}, \quad i = 1, 2, \quad (4)$$

where N is the number of turns of the coil of each electromagnet. Next, we introduce the *generalized voltage* V such that

$$\Delta\dot{\Phi} = \frac{V}{N} \quad (5)$$

and we define the non-dimensionalized state and control variables $x_1 = x/g_0$, $x_2 = \dot{x}/\Phi_{\text{sat}}\sqrt{g_0/\kappa}$, $x_3 = \Delta\Phi/\Phi_{\text{sat}}$, $v = V\sqrt{g_0\kappa}/N\Phi_{\text{sat}}^2$ along with the non-dimensionalized time $\tau = t\Phi_{\text{sat}}/\sqrt{g_0\kappa}$ where g_0 is the nominal air-gap and Φ_{sat} is the value of the saturation (maximum) flux. Then one obtains the following system in state-space form

$$x_1' = x_2 \quad (6a)$$

$$x_2' = \varepsilon x_3 + x_3|x_3| := \varepsilon x_3 + \phi(x_3) \quad (6b)$$

$$x_3' = v \quad (6c)$$

where $\varepsilon = 2\Phi_0/\Phi_{\text{sat}}$ ($0 \leq \varepsilon \ll 1$) and where prime denotes differentiation with respect to the new independent variable τ . Notice that for $\varepsilon = 0$ this model

¹In (4) the coil resistance has been neglected for simplicity.

reduces to the zero bias case. Zero-bias control design for AMBs is especially challenging because of the loss of linear controllability when $\varepsilon = 0$. Reference [14] presents a complete analysis of the zero-bias AMB control problem.

In this paper we are primarily interested in the case where the maximum value of v is limited due to voltage saturation. If, for instance, it is known that $|V| \leq V_{\text{max}}$ then (6c) must be replaced with

$$x_3' = \text{sat}_\lambda(v) := \lambda \text{sat}\left(\frac{v}{\lambda}\right) \quad (7)$$

where $\lambda = V_{\text{max}}\sqrt{g_0\kappa}/N\Phi_{\text{sat}}^2$. For notational simplicity, henceforth we use a dot to denote differentiation with respect to τ .

3 Passivation Design

In this section we develop a passivation design to stabilize the low-bias AMB system (6). Our design starts with the preliminary feedback

$$v = -k_2 x_2 - k_3 x_3 + u, \quad k_2, k_3 > 0. \quad (8)$$

As shown below this feedback law (with $u = 0$) renders the equilibrium $x = 0$ stable with a Lyapunov function V satisfying $\dot{V} \leq 0$. To compute such a V we introduce the new variable

$$z := k_2 x_1 + (k_3/\varepsilon)x_2 + x_3, \quad (9)$$

and rewrite the system (6)-(8) as

$$\dot{z} = \frac{k_3}{\varepsilon} x_3 |x_3| + u \quad (10a)$$

$$\dot{x}_2 = \varepsilon x_3 + x_3 |x_3| \quad (10b)$$

$$\dot{x}_3 = -k_2 x_2 - k_3 x_3 + u. \quad (10c)$$

Then the choice

$$V(z, x_2, x_3) = \varepsilon^2 \int_0^z \text{sat}(s) ds + \frac{k_2}{2} x_2^2 + \frac{\varepsilon}{2} x_3^2 + \frac{1}{3} |x_3| x_3^2$$

satisfies

$$\begin{aligned} \dot{V} &= \varepsilon \text{sat}(z) k_3 x_3 |x_3| - \varepsilon k_3 x_3^2 - k_3 x_3^2 |x_3| \\ &+ (\varepsilon^2 \text{sat}(z) + \varepsilon x_3 + x_3 |x_3|) u \\ &\leq -k_3 x_3^2 |x_3| + (\varepsilon^2 \text{sat}(z) + \varepsilon x_3 + x_3 |x_3|) u, \end{aligned} \quad (11)$$

which means that the system (10) with input u and output $y = \varepsilon^2 \text{sat}(z) + \varepsilon x_3 + x_3 |x_3|$ is passive. With $u = 0$, the origin $x = 0$ is stable but not asymptotically stable, because the system (10) has a continuum of equilibria at $(z_0, 0, 0)$, $z_0 \in \mathfrak{R}$. To increase the negativity in (11) we apply the feedback

$$u = -\text{sat}_\lambda(y) = -\text{sat}_\lambda(\varepsilon^2 \text{sat}(z) + \varepsilon x_3 + x_3 |x_3|)$$

which ensures global asymptotic stability for any saturation level $\lambda > 0$.

Theorem 1 Consider the system (6), and let the variable z be as in (9). Then, the control law

$$v = -k_2 x_2 - k_3 x_3 - \text{sat}_\lambda(\varepsilon^2 \text{sat}(z) + \varepsilon x_3 + x_3 |x_3|) \quad (12)$$

where $k_2, k_3, \lambda > 0$, globally asymptotically stabilizes the origin $x = 0$.

Proof: The result follows from (11) and a straightforward application of LaSalle's invariance principle. ■

4 Small Gain Design

Our next design makes use of an asymptotic small gain theorem by Teel [13]. Before presenting the main result from [13] used herein, we let $|y| := \max_i |y_i|$ denote the norm for a vector $y \in \mathbb{R}^n$, and for a signal $y(t)$, we denote $\|y\|_a = \lim_{t \rightarrow \infty} \sup |y(t)|$. The following result, adapted from [13, Theorem 3], is instrumental in our design:

Proposition 1 *Consider the system*

$$\dot{x} = Ax + Bu + w \quad (13a)$$

$$\dot{z} = f(z, u, d) \quad (13b)$$

$$w = g(z, u, d) \quad (13c)$$

where $x \in \mathbb{R}^{n_1}$, $z \in \mathbb{R}^{n_2}$, A is marginally stable; that is, there exists a matrix $P = P^T > 0$ satisfying $A^T P + PA \leq 0$, the function $f(z, u, d)$ is locally Lipschitz, and the function $g(z, u, d)$ is continuous satisfying

$$\lim_{|(z,u)| \rightarrow 0} \frac{|g(z, u, 0)|}{|(z, u)|} = 0. \quad (14)$$

Suppose, for the z -subsystem (13), there exists a locally Lipschitz class- \mathcal{K} function $\gamma_1(\cdot)$ such that, for each bounded $u(t)$ and $d(t)$, the solution $z(t)$ exists for all $t \in [0, \infty)$, and

$$\|z\|_a \leq \gamma_1(\|u\|_a + \|d\|_a). \quad (15)$$

Then, there exist positive constants Δ and λ^* such that, for each bounded $d(t)$ satisfying $\|d\|_a \leq \Delta$, and for each $\lambda \in (0, \lambda^*]$, the control law

$$u = -\text{sat}_\lambda(B^T P x + d), \quad (16)$$

perturbed by d , ensures that the closed-loop solutions $(x(t), z(t))$ are bounded, and

$$\|(x, z)\|_a \leq \gamma_2(\|d\|_a) \quad (17)$$

for some class- \mathcal{K} function $\gamma_2(\cdot)$. \square

An advantage of the saturation design (16) is that it guarantees robustness against small measurement disturbances d . When the disturbance converges to zero, that is, when $\|d\|_a = 0$, then (17) implies $\|(x, z)\|_a = 0$, which means that the trajectories $(x(t), z(t))$ converge to the origin.

We now apply this design methodology to the AMB system (6). Here we assume that there are no measurement disturbances, i.e., $d(t) \equiv 0$, and we design a globally asymptotically stabilizing control law as in (16). In Section 6 we will implement this control law with state estimates obtained from an observer, and prove stability using the robustness property (17), where d is the observer error.

With the preliminary feedback (8), the (x_2, x_3) -subsystem plays the role of the z -subsystem in Proposition 1 because, as we prove in Theorem 2 below, it satisfies the gain property (15). Next, we note that the system (6)-(8) is of the form (13a) with

$$A = \begin{bmatrix} 0 & 1 & 0 \\ 0 & 0 & \varepsilon \\ 0 & -k_2 & -k_3 \end{bmatrix}, \quad B = \begin{bmatrix} 0 \\ 0 \\ 1 \end{bmatrix}, \quad w = \begin{bmatrix} 0 \\ x_3 |x_3| \\ 0 \end{bmatrix}. \quad (18)$$

The design in Proposition 1 is now applicable because A is marginally stable, and $g(z, u, d)$, given by w above, satisfies (14).

Theorem 2 *For the system (6), let A and B be as in (18) with design parameters $k_2, k_3 > 0$, and let $P = P^T > 0$ be such that $A^T P + PA \leq 0$. Then, there exists a constant λ^* such that, for every $\lambda \in (0, \lambda^*]$, the control law*

$$v = -k_2 x_2 - k_3 x_3 - \text{sat}_\lambda(B^T P x) \quad (19)$$

globally asymptotically stabilizes the equilibrium $x = 0$.

Proof: We first note that the Jacobian linearization of the closed-loop system is $\dot{x} = (A - BB^T P)x$, where $A - BB^T P$ is Hurwitz because (A, B) is controllable. Thus, the equilibrium $x = 0$ is locally asymptotically stable. To prove global attractivity of $x = 0$, we employ Proposition 1 and show that the z -subsystem, rewritten here as

$$\begin{aligned} \dot{x}_2 &= \varepsilon x_3 + x_3 |x_3| \\ \dot{x}_3 &= -k_2 x_2 - k_3 x_3 + u, \end{aligned} \quad (20)$$

satisfies the gain condition (15). To this end, we let

$$V = \frac{k_2}{2} x_2^2 + \frac{\varepsilon}{2} x_3^2 + \mu x_2 x_3 + \frac{1}{3} |x_3| x_3^2 \quad (21)$$

where $0 < \mu < \min\{k_3, \sqrt{k_2 \varepsilon}, 4\varepsilon k_2 k_3 / (4\varepsilon k_2 + k_3^2)\}$. It can be readily shown that V is positive definite. The derivative of V along the trajectories of (20) is

$$\begin{aligned} \dot{V} &= -\varepsilon \bar{\mu} x_3^2 - k_2 \mu x_2^2 - \mu k_3 x_2 x_3 \\ &\quad - \bar{\mu} |x_3| x_3^2 + \varepsilon x_3 u + u |x_3| x_3 + \mu x_2 u \\ &\leq -a_1 |x|^2 + (\varepsilon + \mu) |x| |u| + |u| |x_3|^2 - \bar{\mu} |x_3|^3 \end{aligned}$$

where $a_1 = \frac{1}{2}(\varepsilon \bar{\mu} + \mu k_2 - \sqrt{(\varepsilon \bar{\mu} - \mu k_2)^2 + \mu^2 k_3^2}) > 0$ and $\bar{\mu} = k_3 - \mu$. Using Young's inequality [8, p. 75] we have

$$|u| |x_3|^2 \leq \frac{4}{27} \frac{1}{\bar{\mu}^2} |u|^3 + \bar{\mu} |x_3|^3$$

Thus,

$$\dot{V} \leq -a_1 |x|^2 + a_2 |x| |u| + a_3 |u|^3 \quad (22)$$

where $a_2 = \varepsilon + \mu$ and $a_3 = 4/27 \bar{\mu}^2$. Upon completion of squares, the last inequality yields

$$\dot{V} \leq -(a_1 - \frac{a_2^2}{2} b) |x|^2 + \frac{a_2}{2\kappa} |u|^2 + a_3 |u|^3 \quad (23)$$

where b a positive number such that $b < 2a_1/a_2$. From (23) it follows that $\dot{V} < 0$ whenever $|x| > \sqrt{c_1 |u|^2 + c_2 |u|^3} = \rho(|u|)$ with $c_1 = a_2/b(2a_1 - a_2b)$ and $c_2 = 2a_3/(2a_1 - a_2b)$. Now let $c_3 = \frac{1}{2}(k_2 + \varepsilon - \sqrt{(k_2 - \varepsilon)^2 + 4\mu^2})$ and $c_4 = k_2 + \varepsilon + \sqrt{(k_2 - \varepsilon)^2 + 4\mu^2}$ and note that

$$\underline{\alpha}(|x|) = c_3 |x|^2 \leq V(x) \leq c_4 |x|^2 + \frac{1}{3} |x|^3 = \bar{\alpha}(|x|).$$

Using [3, Fact 37] we conclude that

$$\|(x_2, x_3)\|_a \leq \gamma_1(\|u\|_a) \quad (24)$$

where $\gamma_1(s) = \frac{\underline{\alpha}^{-1}(\bar{\alpha}(\rho(s)))}{\sqrt{b_1 s^2 + b_2 s^3 + (b_3 s^2 + b_4 s^3)^{3/2}}}$, $b_1 = c_4 c_1 / c_3$, $b_2 = c_4 c_2 / c_3$, $b_3 = c_1 / (3c_3)^{2/3}$, $b_4 = c_2 / (3c_3)^{2/3}$. Thus, from Proposition 1, the solution $x(t)$ exists for all $t \in [0, \infty)$, and $\|x\|_a = 0$, that is, the equilibrium $x = 0$ is globally attractive. \blacksquare

5 Nested Saturation Design

The control laws (12) and (19) are only partially saturated. We now design a completely saturated control law following the *nested saturation* scheme of Teel [12]. Unlike the general procedure in [12], in the following proposition we explicitly compute admissible saturation levels.

Proposition 2 *Consider the system (6). The control law*

$$v = -\text{sat}_{\lambda_1}(x_3 + \text{sat}_{\lambda_2}(\frac{x_2}{\varepsilon} + x_3 + \text{sat}_{\lambda_3}(\frac{x_1}{\varepsilon} + \frac{2}{\varepsilon}x_2 + x_3))) \quad (25)$$

with $\lambda_1 > 0$ and

$$0 < \lambda_2 < \min\{\frac{\lambda_1}{2}, \frac{\varepsilon}{5}\}, \quad \frac{2}{\varepsilon}\lambda_2^2 < \lambda_3 < \frac{1}{2}(\lambda_2 - \frac{1}{\varepsilon}\lambda_2^2) \quad (26)$$

globally asymptotically stabilizes the equilibrium $x = 0$.

Proof: With $y_3 := x_3$, $y_2 := (x_2/\varepsilon) + x_3$, and $y_1 := (x_1/\varepsilon) + (2/\varepsilon)x_2 + x_3$, the closed-loop system (6),(25), is rewritten as

$$\dot{y}_1 = y_2 + y_3 + v + (2/\varepsilon)y_3|y_3| \quad (27a)$$

$$\dot{y}_2 = y_3 + v + \frac{1}{\varepsilon}y_3|y_3| \quad (27b)$$

$$\dot{y}_3 = v = -\text{sat}_{\lambda_1}(y_3 + v_2), \quad (27c)$$

where $v_2 = \text{sat}_{\lambda_2}(y_2 + \text{sat}_{\lambda_3}(y_1))$. First, we note from the *feedforward* structure that the closed-loop system does not exhibit finite escape time. Next, because $|v_2| \leq \lambda_2$ in (27c), the Lyapunov function $V_3 = \frac{1}{2}y_3^2$ satisfies $\dot{V}_3 < 0$ whenever $|y_3| > \lambda_2$ and, hence $\|y_3\|_a \leq \lambda_2$. Using $\lambda_2 < \lambda_1/2$, it follows that the saturation function $\text{sat}_{\lambda_1}(y_3 + v_2)$ operates in its linear region after a finite time t_1 . Thus, for $t \geq t_1$,

$$v = -y_3 - v_2 = -y_3 - \text{sat}_{\lambda_2}(y_2 + \text{sat}_{\lambda_3}(y_1)), \quad (28)$$

and the y_2 -subsystem is

$$\dot{y}_2 = -\text{sat}_{\lambda_2}(y_2 + v_3) + w_2 \quad (29)$$

where $v_3 = \text{sat}_{\lambda_3}(y_1)$ and $w_2 = \frac{1}{\varepsilon}y_3|y_3|$. Using the Lyapunov function $V_2 = \frac{1}{2}y_2^2$ one can show that $\dot{V}_2 < 0$ whenever $|w_2| < \lambda_2$ and $|y_2| > |v_3| + |w_2|$. Because $\|w_2\|_a \leq \frac{1}{\varepsilon}\|y_3\|_a^2 \leq \frac{1}{\varepsilon}\lambda_2^2 < \lambda_2$ from (26), it follows that $\|y_2\|_a \leq \|v_3\|_a + \|w_2\|_a$. From this inequality and using $\|v_3\|_a \leq \lambda_3$, $\|w_2\|_a \leq \frac{1}{\varepsilon}\lambda_2^2$ and the last inequality in (26), it is not difficult to show that $\|y_2\|_a + \|v_3\|_a < \lambda_2$; that is, after a finite time $t_2 \geq t_1$, $v_2 = \text{sat}_{\lambda_2}(y_2 + v_3) = y_2 + v_3$ which implies that $v = -y_2 - y_3 - \text{sat}_{\lambda_3}(y_1)$. This means that, for $t \geq t_2$, the y_1 -subsystem is

$$\dot{y}_1 = -\text{sat}_{\lambda_3}(y_1) + w_3 \quad (30)$$

where $w_3 = (2/\varepsilon)y_3|y_3|$. We first note that a λ_3 satisfying the last inequality in (26) exists because $\lambda_2 < \varepsilon/5$ in the second inequality. Next, because $\lambda_3 > 2\lambda_2^2/\varepsilon$, it follows from (30) that $\|y_1\|_a \leq \|w_3\|_a \leq (2/\varepsilon)\lambda_2^2 < \lambda_3$,

which means that, after a finite time t_3 , $\text{sat}_{\lambda_3}(y_1) = y_1$. Thus, for $t \geq t_3 \geq t_2$, the closed-loop system is

$$\dot{y}_1 = -y_1 + (2/\varepsilon)y_3|y_3| \quad (31a)$$

$$\dot{y}_2 = -y_1 - y_2 + (1/\varepsilon)y_3|y_3| \quad (31b)$$

$$\dot{y}_3 = -y_2 - y_2 - y_3. \quad (31c)$$

We conclude the proof by showing that this system is globally asymptotically stable. Indeed, the derivative of the Lyapunov function

$$V = 3y_1^2 - 4y_1y_2 + 8y_2^2 + (8/3\varepsilon)y_3|y_3|^2 \quad (32)$$

along the trajectories of (31) is

$$\dot{V} = -2y_1^2 - 8y_1y_2 - 16y_2^2 - (8/\varepsilon)y_3|y_3|^2, \quad (33)$$

which is negative definite. Thus, the system (6), (25) is globally asymptotically stable. ■

6 Flux Observer Design and Output Feedback

Thus far, our designs relied on the availability of flux measurements, which may be difficult in practice [5]. Because the system nonlinearity $\phi(x_3) = x_3|x_3|$ in (6) is non-decreasing, we pursue the observer design of Arcak and Kokotović [1] for this class of nonlinearities. When ε is small as in low bias applications, a full-order design gives rise to large observer transients. We circumvent this problem with a reduced-order variant of the observer in [1]:

Proposition 3 *Consider the system (6) with the output $y = x_2$, and define the new variable $\chi := x_3 - (k/\varepsilon)y$ where $k > 0$ is a design parameter. With the reduced-order observer*

$$\dot{\hat{\chi}} = v - k(\hat{\chi} + \frac{k}{\varepsilon}y) - \frac{k}{\varepsilon}\phi(\hat{\chi} + \frac{k}{\varepsilon}y) \quad (34a)$$

$$\hat{x}_3 = \hat{\chi} + \frac{k}{\varepsilon}y, \quad (34b)$$

the observer error $d(t) := \hat{x}_3(t) - x_3(t)$ satisfies, for all t in the maximal interval of existence $[0, t_f)$ of (6), (34),

$$|d(t)| \leq |d(0)|e^{-kt}. \quad (35)$$

Proof: First, notice that the observation error $d = \hat{\chi} - \chi$ satisfies

$$\dot{d} = \dot{\hat{\chi}} - \dot{\chi} = -kd - \frac{k}{\varepsilon} \left[\phi(\hat{\chi} + \frac{k}{\varepsilon}y) - \phi(\chi + \frac{k}{\varepsilon}y) \right]. \quad (36)$$

Next, because the function $\phi(x_3) = x_3|x_3|$ is non-decreasing, we get

$$(\hat{\chi} - \chi) \left[\phi(\hat{\chi} + \frac{k}{\varepsilon}x_2) - \phi(\chi + \frac{k}{\varepsilon}x_2) \right] \geq 0, \quad (37)$$

from which the derivative of $V = \frac{1}{2}d^2$ satisfies $\dot{V} = -kd^2 = -2kV$, thus proving (35). ■

Theorem 3 Consider the system (6) and the observer (34). Either one of the control laws (12), (19), or (25), implemented with \hat{x}_3 instead of x_3 , globally asymptotically stabilizes the origin $(x, \hat{x}) = 0$.

Proof: We first prove stability for the passivation design (12). When x_3 is replaced with $\hat{x}_3 = x_3 + d$, the resulting output feedback control law \tilde{v} differs from the state feedback control law v in (12), by

$$\begin{aligned} \tilde{d} := v - \tilde{v} &= k_3 d + \text{sat}_\lambda(\varepsilon^2 \text{sat}(z + d) \\ &+ \varepsilon(x_3 + d) + (x_3 + d)|x_3 + d|) \\ &- \text{sat}_\lambda(\varepsilon^2 \text{sat}(z) + \varepsilon x_3 + x_3|x_3|). \end{aligned}$$

Then, the derivative of the Lyapunov function (3), along the trajectories of (6) with \tilde{v} , satisfies

$$\dot{V} \leq -k_3|x_3|^3 - (\varepsilon^2 \text{sat}(z) + \varepsilon x_3 + x_3|x_3|)\tilde{d}. \quad (38)$$

Using the inequalities $x_3|x_3|\tilde{d} \leq (k_3/4)|x_3|^3 + (4/k_3)^2|\tilde{d}|^3$ (to see this, consider the two cases $|\tilde{d}| \leq (k_3/4)|x_3|$ and $|x_3| \leq (4/k_3)|\tilde{d}|$), and $\varepsilon x_3 \tilde{d} \leq (k_3/4)|x_3|^3 + \varepsilon|\tilde{d}|\sqrt{(4\varepsilon/k_3)|\tilde{d}|}$ (consider the two cases $|\tilde{d}| \leq (k_3/4\varepsilon)|x_3|^2$ and $|x_3| \leq \sqrt{(4\varepsilon/k_3)|\tilde{d}|}$), we obtain

$$\dot{V} \leq -\frac{k_3}{2}|x_3|^3 + \left[\varepsilon^2|\tilde{d}| + \left(\frac{4}{k_3}\right)^2|\tilde{d}|^3 + \varepsilon|\tilde{d}|\sqrt{\frac{4\varepsilon}{k_3}|\tilde{d}|} \right].$$

Next, letting T be in the maximal interval of existence $[0, t_f)$ of the closed-loop system and integrating both sides of (6) from 0 to T , we obtain

$$V(x(T)) - V(x(0)) \leq \int_0^T \left[\varepsilon^2|\tilde{d}| + \left(\frac{4}{k_3}\right)^2|\tilde{d}|^3 + \varepsilon|\tilde{d}|\sqrt{\frac{4\varepsilon}{k_3}|\tilde{d}|} \right] dt. \quad (39)$$

Because \tilde{d} is exponentially decaying from (35) and (6), the integral on the right-hand side has an upper-bound which is independent of T . This proves that $t_f = \infty$, and the trajectories are bounded. Finally, because \tilde{d} converges to zero, it follows from LaSalle's invariance principle that the solutions converge to the largest invariant set where $d = 0$. When $d = 0$, the output feedback control law coincides with the state feedback control law and, hence, the largest invariant set is the origin. This concludes the proof of global asymptotic stability for the passivation design (12).

When the small gain design (19) is implemented with \hat{x}_3 , the closed-loop system is

$$\dot{\hat{x}}_1 = x_2 \quad (40a)$$

$$\dot{\hat{x}}_2 = \varepsilon x_3 + x_3|x_3| \quad (40b)$$

$$\dot{\hat{x}}_3 = -k_2 x_2 - k_3(x_3 + d) - \text{sat}_\lambda(B^T P \hat{x}) \quad (40c)$$

where $\hat{x} = [x_1 \ x_2 \ \hat{x}_3]^T$. To show that there is no finite escape time, we assume $t_f < \infty$ and let $T \in [0, t_f)$. The arguments used in the proof of Theorem 2 show that the (x_2, x_3) subsystem is *input-to-state stable* [11, Lemma 2.14] with respect to the disturbance $\tilde{u} = -k_3 d - \text{sat}_\lambda(B^T P \hat{x})$; that is, for all $t \in [0, T]$,

$$|(x_2(t), x_3(t))| \leq \beta(|(x_2(0), x_3(0))|, t) + \gamma\left(\sup_{t \in [0, T]} |\tilde{u}|\right). \quad (41)$$

where $\beta(\cdot, \cdot)$ is a class- \mathcal{KL} function and $\gamma(\cdot)$ is a \mathcal{K} -class function. Since $\beta(\cdot, t)$ is a decreasing function in t and because $|d(t)| \leq |d(0)|$ and $|\text{sat}_\lambda(B^T P \hat{x}(t))| \leq \lambda$, it follows from (41) that, in the interval $t \in [0, T]$, $|(x_2(t), x_3(t))|$ is bounded by a function of initial conditions that is independent of T . Likewise, using $\dot{x}_1 = x_2$ and (41), we conclude that $|x_1(t)|$ has an upper bound which is a continuous function of T , which contradicts the assumption $t_f < \infty$ because T can be arbitrarily close to t_f .

To prove stability of the equilibrium $(x, d) = 0$, we represent the closed-loop system (40) as in Proposition 1, where the z -subsystem is as in (20), with u replaced with $\tilde{u} = u - k_3 d$, and

$$w = g(z, u, d) = \begin{bmatrix} 0 \\ x_3|x_3| \\ -k_3 d \end{bmatrix} \quad (42)$$

in (18). Then, the same argument as in Theorem 2 implies that (24) holds for $\tilde{u} = u - k_3 d$ and, from $\|\tilde{u}\|_a \leq \max\{1, k_3\}(\|u\|_a + \|d\|_a)$, the gain condition (15) of Proposition 1 holds. Because $\|d\|_a = 0$, it follows from (17) that the equilibrium $(x, d) = 0$ is globally attractive. Finally, it is not difficult to show from the Jacobian linearization that the equilibrium is also stable. Having established stability and attractivity, we conclude that the equilibrium is globally asymptotically stable.

The proof of stability for the nested saturation design (25) is straightforward because the arguments in the proof of Proposition 2 continue to hold when x_3 is replaced with $\hat{x}_3 = x_3 + d$ where $\|d_a\| = 0$. ■

7 Numerical Examples

In this section we illustrate the previous theoretical results via a series of numerical simulations. Due to space limitation only the results for controllers (12) and (19) are shown here. We consider a magnetic bearing with characteristics similar to those in Ref. [6]. The bias voltage is chosen as $\Phi_0 = 10 \mu\text{Wb}$. This corresponds to $\varepsilon = 0.1$ and it is an order of magnitude less than what is typically used in practice². The results of the simulations with the control law (12) for two different values of voltage saturation $V_{\max} = 10 \text{ V}$ and $V_{\max} = 1 \text{ V}$ are shown in Figs. 2. In all cases, the observer in (34) was implemented to estimate the flux. Simulations with several values of the observer gain k were performed. As shown in Fig. 2 the trajectories of the observer-controller interconnection tend to the trajectories of the state-feedback controller with increasing k .

The results of the simulations with the control law (19) for $V_{\max} = 10 \text{ V}$ and $V_{\max} = 5 \text{ V}$ are shown in Figs. 3. Simulations with other saturation levels and initial conditions give similar results.

²A value of 40-50% of the saturation flux is used for most typical biasing schemes.

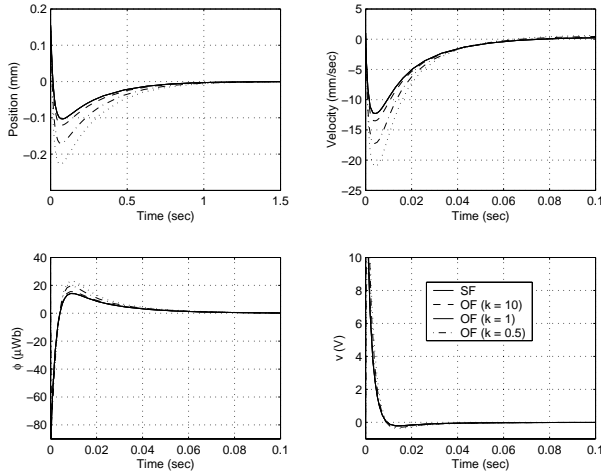


Figure 2: State-feedback and output-feedback system trajectories with control law (12) and different observer gains: $k = 0.5, k = 1, k = 10$. Controller gains $k_2 = k_3 = 1$.

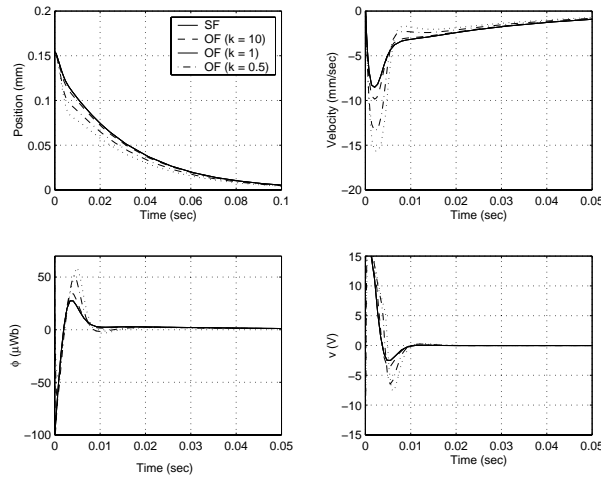


Figure 3: State-feedback and output-feedback system trajectories with control law (19) and different observer gains: $k = 0.5, k = 1, k = 10$. Controller gains $k_2 = k_3 = 1$.

8 Conclusions

Low-bias control of an active magnetic bearing subject to voltage saturation is a challenging control problem. In this paper we have presented three different flux-based designs for low-bias operation of active magnetic bearings using ideas from passivity, the asymptotic small-gain theorem of Teel, and nonlinear saturated control. Since flux is not typically available for feedback we also propose a nonlinear reduced-order observer to estimate the flux from velocity measurements. We have shown that this flux observer, when interconnected in a certainty-equivalence implementation with the state-feedback controllers, results in a globally asymptotically stable system.

Acknowledgments: The authors would like to thank Prof. A. Teel and Prof. E. Maslen for helpful comments during the preparation of this work.

References

- [1] M. Arcak and P. Kokotović, “Observer-Based Control of Systems with Slope-Restricted Nonlinearities,” *IEEE Transactions on Automatic Control*, Vol. 46, 2001.
- [2] A. Charara, J. De Miras, and B. Caron, “Nonlinear Control of a Magnetic Levitation System Without Premagnetization,” *IEEE Transactions on Control Systems Technology*, Vol. 4, No. 5, pp. 513–523, 1996.
- [3] J. M. Coron, L. Praly, and A. Teel, “Feedback Stabilization of Nonlinear Systems: Sufficient Conditions and Lyapunov and Input-Output Techniques,” in *Trends in Control: A European Perspective* (A. Isidori, ed.), pp. 293–348, London: Springer-Verlag, 1995.
- [4] D. Johnson, G. V. Brown, and D. J. Inman, “Adaptive Variable Bias Magnetic Bearing Control,” in *Proceedings of the American Control Conference*, pp. 2217–2223, 1998. Philadelphia, PA.
- [5] F. Keith, *Implicit Flux Feedback Control for Magnetic Bearings*, Ph.D. dissertation, University of Virginia, Charlottesville, Virginia, 1993.
- [6] C. Knospe, “The Nonlinear Control Benchmark Experiment,” in *Proceedings of the American Control Conference*, pp. 2134–2138, 2000. Chicago, IL.
- [7] C. Knospe and C. Yang, “Gain-Scheduled Control of a Magnetic Bearing with Low Bias Flux,” in *Proceedings of the 36th Conference on Decision and Control*, pp. 418–423, 1997. San Diego, CA.
- [8] M. Krstić, I. Kanellakopoulos, and P. Kokotović, *Nonlinear and Adaptive Control Design*, New York: Wiley and Sons, 1995.
- [9] P. Proctor, “Flywheels Show Promise for ‘High-Pulse’ Satellites,” *Aviation Week and Space Technology*, p. 67, January 25 1999.
- [10] N. N. Rao, *Elements of Engineering Electromagnetics, Fourth Edition*, Englewood Cliffs, NJ: Prentice Hall, Inc., 1994.
- [11] E. Sontag and Y. Wang, “On Characterizations of the Input-to-State Stability Property,” *Systems and Control Letters*, Vol. 24, pp. 351–359, 1995.
- [12] A. Teel, “Using saturation to stabilize a class of single-input partially linear composite systems,” in *Preprints of the 2nd IFAC Nonlinear Control Systems Design Symposium*, (Bordeaux, France), pp. 224–229, 1992.
- [13] A. Teel, “A Nonlinear Small Gain Theorem for the Analysis of Control Systems with Saturation,” *IEEE Transactions on Automatic Control*, Vol. 41, No. 9, pp. 1256–1270, 1996.
- [14] P. Tsiotras, B. Wilson, and R. Bartlett, “Control of a Zero-Bias Magnetic Bearing Using Control Lyapunov Functions,” in *39th IEEE Conference on Decision and Control*, pp. 4048–4053, 2000. Sydney, Australia.